Nanoscale Cellular Changes in Field Carcinogenesis Detected by Partial Wave Spectroscopy

Harihara Subramanian,[1] Hemant K. Roy,[2] Prabhakar Pradhan,[1] Michael J. Goldberg,[2] Joseph Muldoon,[2] Randall E. Brand,[2] Charles Sturgis,[2] Thomas Hensing,[2] Daniel Ray,[2] Andrej Bogojevic,[2] Jameel Mohammed,[2] Jeen-Soo Chang,[2] and Vadim Backman[1]

[1]Biomedical Engineering Department, Northwestern University and [2]Department of Internal Medicine, Northshore University HealthSystem, Evanston, Illinois

Abstract

Understanding alteration of cell morphology in disease has been hampered by the diffraction-limited resolution of optical microscopy (>200 nm). We recently developed an optical microscopy technique, partial wave spectroscopy (PWS), which is capable of quantifying statistical properties of cell structure at the nanoscale. Here we use PWS to show for the first time the increase in the disorder strength of the nanoscale architecture not only in tumor cells but also in the microscopically normal-appearing cells outside of the tumor. Although genetic and epigenetic alterations have been previously observed in the field of carcinogenesis, these cells were considered morphologically normal. Our data show organ-wide alteration in cell nanoarchitecture. This seems to be a general event in carcinogenesis, which is supported by our data in three types of cancer: colon, pancreatic, and lung. These results have important implications in that PWS can be used as a new method to identify patients harboring malignant or premalignant tumors by interrogating easily accessible tissue sites distant from the location of the lesion. [Cancer Res 2009;69(13):5357–63]

Introduction

Epithelial dysplasia (microscopic abnormalities associated with malignant transformation) and cancer are the culmination of a protracted process of genetic and epigenetic events. Thus, it is well established that in the microscopically normal mucosa undergoing neoplastic transformation, there is profound activation of proto-oncogenes (through mutation or increased copy number) or loss of tumor suppressor genes (via both mutations or through epigenetic silencing by promoter hypermethylation, microRNA or histone acetylation). Furthermore, it is being increasingly recognized that these genetic and epigenetic alterations occur not only at the neoplastic focus but more diffusely (field cancerization).

Neoplastic transformation of the colon is a prototypical example of field carcinogenesis. Indeed, the knowledge of field carcinogenesis has been used for clinical practice via the flexible sigmoidoscopy. This approach is based on the fact that endoscopic detection of adenomas in the distal colon portends a ∼2.5-fold excess risk of proximal neoplasia (1). Numerous other biomarkers of colon carcinogenesis have been shown to correlate with the presence of neoplasia, including morphologic [aberrant crypt foci (2)], cellular [altered proliferation (3) and apoptosis (4)], and molecular [genomic, methylation, and proteomic (5–8)]. Many of these markers are detected in mucosa that is classified as normal by light microscopy. Whereas one would anticipate that these genetic/epigenetic changes would result in structural changes, the diffraction-limited resolution of light renders the conventional microscopy to be insensitive to structures <200 nm, which would include ribosomes, macromolecular complexes, nucleosomes, membranes, etc. These nanoscale structures are some of the most fundamental building blocks of a cell and are the most likely to be altered in early neoplastic transformation. Indeed, techniques such as karyometry have suggested that there are subtle ultrastructural alterations as markers of field cancerization (9, 10). However, the ability to sensitively and robustly detect these changes has been heretofore impossible. We posed a question if in early carcinogenesis microscopically normal-appearing cells do posses alterations in their morphology, although these changes occur at length scales not accessible by conventional microscopy (i.e., nano-architecture).

To assess the nanoscale, we have used a fundamental principle of mesoscopic light transport theory (11–15) that the signal in one dimension arising due to multiple interferences of light waves reflected from weak refractive index fluctuations is sensitive to any length scale of refractive index fluctuations. Therefore, the spectrum of the one-dimensional scattering signals contains information about particles whose length scales are well below the wavelength (≪200 nm; refs. 16–18). We recently reported a novel optical technique, partial wave spectroscopy (PWS), that is capable of extracting one-dimensional propagating waves (partial waves) from different parts of a scattering particle (19). We have also recently shown that PWS was sensitive to subtle genetic/epigenetic alterations that occur in colonic carcinogenesis (20). Moreover, in the multiple intestinal neoplasia (MIN) model, the abnormalities detected using PWS preceded the development of microscopically evident neoplasia, further supporting its role in field carcinogenesis detection. In this study, we show that these findings observed earlier in human colon cell lines and MIN mouse model are translatable to the detection of human colorectal carcinogenesis. Our results also indicate that PWS may have the promise for detecting extended field carcinogenesis in the pancreas and lung.

Materials and Methods

Partial Wave Spectroscopic Microscopy

The design of the PWS instrument is discussed in detail elsewhere (20). In brief, a nearly plane wave of white, low-spatially coherent light illuminates the sample and an image formed by the backscattered photons is acquired. The spectra of the backscattered light within the wavelength

Cancer Research

range of 400 to 700 nm are acquired from each pixel, normalized by the spectrum of the incident light, and filtered to remove spectral noise. This yields a data cube $R(\lambda, x, y)$, where λ is the wavelength and x and y are pixel coordinates, which is referred to as the fluctuating part of the reflection coefficient. Hence, unlike conventional microscopy, in which an image is formed by integrating the reflected or transmitted intensity over a broad spectrum, PWS measures spectral fluctuations in the backscattering spectra. In essence, PWS decomposes a complex three-dimensional weakly disordered medium such as a biological cell into many spatially independent parallel one-dimensional channels, each with diffraction-limited transverse size, and acquires one-dimensional reflection spectra $R(\lambda; x, y)$. These spectral fluctuations are analyzed by means of one-dimensional mesoscopic light transport theory. This theory enables quantification of the statistical properties of the spatial refractive index variations at any length scale including those well below the wavelength ($\ll 200$ nm). The statistical parameter determined from the analysis is the disorder strength $L_d = \langle \Delta n^2 \rangle l_c$, where $\langle \Delta n^2 \rangle$ and l_c are the variance and the spatial correlation length of the refractive index fluctuations. At a given point in a cell, Δn is proportional to the local concentration of intracellular solids and l_c is related to the size of the intracellular structures within a cell. We had recently shown using numerical simulations and model experiments that the minimum l_c that can be probed by using PWS is <20 nm (20, 21). Thus, using PWS, a two-dimensional map depicting the distribution of disorder strength $L_d(x,y)$ can be obtained for a particular cell. From these two-dimensional images, several statistical parameters can be extracted, such as the mean intracellular disorder strength $L_d^{(c)}$ [the average $L_d(x,y)$ over x and y] and the SD of intracellular disorder strength, $\sigma^{(c)}$. The averages of $L_d^{(c)}, \sigma^{(c)}$ over a group of cells, such as cells sampled from a particular patient category, are termed the group means $L_d^{(g)}$ and $\sigma^{(g)}$.

The stability of the PWS instrument was established by calculating the statistical parameters $L_d^{(c)}$ and $\sigma^{(c)}$ from a cell sample at different time points on the same day. This technical reproducibility of the PWS instrument was measured to be ~1.5%. In addition, the variability of the statistical parameters from the same sample measured over a period of 30 d was measured to be ~5%. This measure included both the variability of the system and the sample over a period of 30 d. The variability of disorder strength calculated from multiple cytologic samples of the same patient was ~25%, which probably reflects the "patchiness" of the field effect (22, 23).

Human Studies

All studies were done and the samples were collected with the approval of the institutional review board at Northshore University HealthSystem.

Colon. Patients undergoing screening or surveillance colonoscopy scheduled at Northshore University Health System were included in the study. The exclusion criteria included incomplete colonoscopy (failure to intubate cecum), poor colonic preparation, coagulopathy, prior history of pelvic radiation, or systemic chemotherapy. The samples were collected as follows: Colonoscopy to cecum was done with standard techniques using Olympus 160 or 180 series colonoscopes. On withdrawal of the colonoscope to the rectum, a cytology brush was passed through the endoscope and gently applied to the visually normal rectum.

Pancreas. The controls are patients undergoing esophagogastroduodenoscopy for nonpancreatic reasons. The cancer patients are patients with histologically confirmed pancreatic cancer undergoing endoscopic ultrasound or endoscopic retrograde pacreatocholangiography. The patients with the history of systemic chemotherapy or radiation therapy, coagulopathy, or failure to obtain histologic confirmation of malignancy were excluded from the study. The samples were collected as follows: An Olympus 180 series upper endoscope was inserted under direct visualization to the second portion of the duodenum. The ampulla was identified and then an endoscopically compatible cytology brush was used to gently sample the endoscopically normal periampullary mucosa.

Lung. Patients with radiographic confirmation of COPD or histologic confirmation of lung malignancy were included in the study, whereas patients with history of systemic chemotherapy or radiation therapy,

coagulopathy, or failure to obtain histologic confirmation of malignancy were excluded from the study. The samples were collected by gently brushing the visually normal buccal mucosa of the patients using a cytologic brush.

The cytology brush obtained from above studies was then applied to a sterile glass slide. The slides were then fixed in an alcohol bath containing 90% ethylalcohol. Although the cytologic slide contained different types of cells including epithelial and inflammatory cells, we note that all the
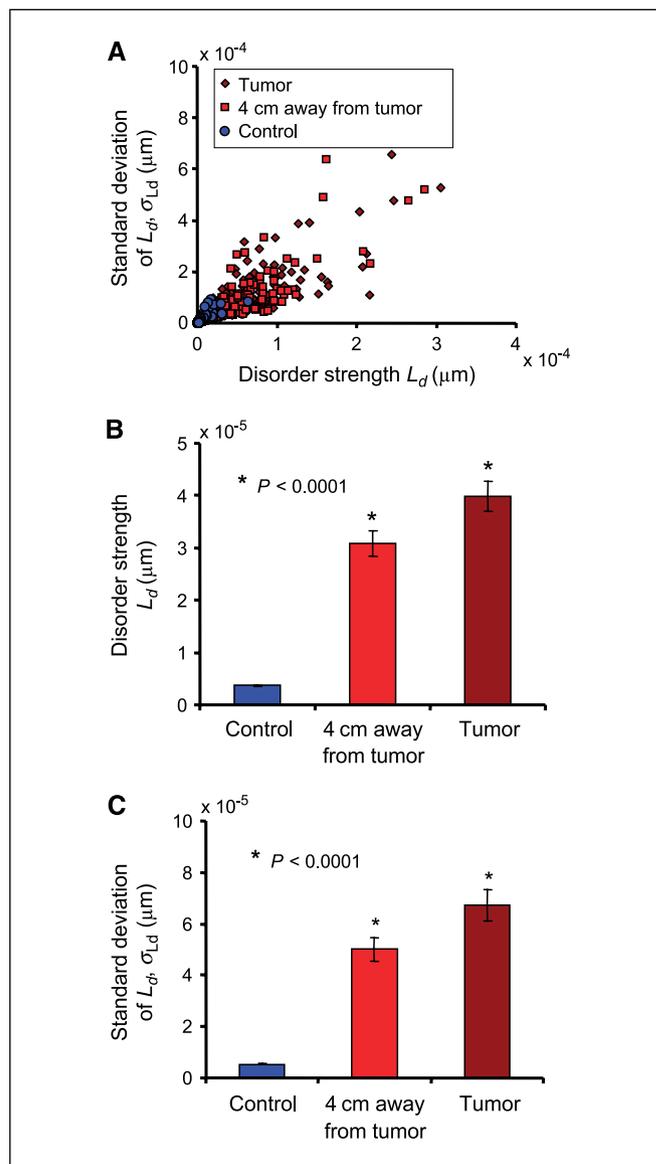

Figure 1. *A,* cells at a distance from a colon tumor undergo changes in their internal nanoarchitecture similar to tumor cells. Values of L_d and its intracellular SD σ_{Ld} averaged over a cell, that is, $L_d^{(c)}$ and $\sigma^{(c)}$, for control cells, tumor cells, and cells at a 4-cm distance from tumor plotted in $L_d^{(c)}, \sigma^{(c)}$ parameter space. Each point in this diagram corresponds to a single cell. As can be seen, the histologically normal cells at a distance from a tumor have an increased disorder strength due to field carcinogenesis. *B,* relative values of the disorder strength $L_d^{(g)}$ for the control cells, tumor cells, and cells away from tumor. $L_d^{(g)}$ is obtained by averaging $L_d^{(c)}$ from randomly chosen ~30 cells for each of the three cell types. *Bars,* SE. The average disorder strength $L_d^{(g)}$ is significantly increased in the tumor cells compared with control cells (Student's *t* test, $P < 0.0001$). More importantly, cells 4 cm away from tumor also undergo increased disorder strength compared with control ($P < 0.0001$). *C,* values of the intracellular SD of the disorder strength $\sigma^{(g)}$ for the three cell types. $\sigma^{(g)}$ is obtained from ~30 cells for each cell type. *Bars,* SE of the means. $\sigma^{(g)}$ is progressively increased in cells 4 cm away from tumor to the tumor cells compared with control (all $P < 0.0001$).

Table 1. Demographic information of the subjects involved in the rectal study and the effect of the patient characteristics on PWS parameters

Demographic factor	Information	Effect on L_d, ANCOVA P	Effect on σ_{Ld}, ANCOVA P
Age (mean $\pm$ SD) y	Control: 59 $\pm$ 9	0.19	0.23
	Adenoma: 58 $\pm$ 11		
	Advanced adenoma: 56 $\pm$ 22		
Smoking (%smokers)	Control: 30%	0.50	0.77
	Adenoma: 27%		
	Advanced adenoma: 75%		
Race (%White)	Control: 100%		
	Adenoma: 100%		
	Advanced adenoma: 100%		
Gender (%male)	Control: 40%	0.89	0.88
	Adenoma: 63%		
	Advanced adenoma: 100%		

NOTE: The table indicates that both $L_d^{(g)}$ and $\sigma^{(g)}$ are not confounded by the patient demographic factors.

measurements mentioned in this article were taken from epithelial cells. This was made possible by directly visualizing the cells before taking the PWS measurements (PWS system contains a flipper mirror that directs the image of a cell into a digital camera for quick visualization).

Statistical Methods

All P values were calculated using Student's t tests. Leave-one-out cross-validation was done with logistic regression in Matlab (Mathworks) by determining values for each patient without including that patient in the fitting model. Contributions of demographic factors toward the PWS parameters [$L_d^{(g)}$ and $\sigma^{(g)}$] were evaluated by performing ANOVA and analysis of covariance (ANCOVA) tests in STATA (Stata Corp.).

Results and Discussion

We first confirmed that PWS could distinguish morphologically normal and abnormal cells by examining cytologic preparations of brushings from colorectal cancer patients (n = 10) and normal patients (n = 20). The normal patients had an average age of 59 $\pm$ 9 years (mean $\pm$ SD) with 40% being male. Similarly, the cancer population had an average age of 71 $\pm$ 13 years with 60% being male. First, we noted that both $L_d^{(c)}$ and $\sigma^{(c)}$ showed no significant difference (P > 0.2, ANOVA) among cancer cells obtained from tumors located at different parts of the colon. Figure 1A plots $L_d^{(c)}$ versus $\sigma^{(c)}$ for all cells for the normal and cancer groups, with each cell being represented by a point [$L_d^{(c)},\sigma^{(c)}$]. Clearly, both $L_d^{(c)}$ and $\sigma^{(c)}$ are increased in cancer cells. This is further illustrated in Fig. 1B and C, which shows that both $L_d^{(g)}$ and $\sigma^{(g)}$ were highly elevated (P < 0.001) in the tumor cells when compared with the cells obtained from normal patients. These results agree well with the conventional cytology in that cancer cells show a significant difference in their morphology compared with the normal cells.

We next study the changes in the internal architecture of the cells outside of the spatial extent of tumors in the field of carcinogenesis. The cells were obtained from the patients with colorectal cancer (n = 10), this time from locations >4 cm away from the tumor. All cells were cytologically normal. The question we asked was as follows: Although appearing normal by the criteria of microscopic histopathology, do these colonocytes possess alterations in their nanoarchitecture? Figure 1B and C shows that both $L_d^{(g)}$ and $\sigma^{(g)}$ are highly significantly (P < 0.001) increased in

the cells obtained from outside the tumor boundary compared with those from normal patients. Interestingly, these cells only had a slightly decreased $L_d^{(g)}$ and $\sigma^{(g)}$ compared with cancer cells. That is, the effect size between controls (no neoplasia) and field carcinogenesis (histologically normal mucosa of patient harboring neoplasia) was much greater than those between the field carcinogenesis and frankly malignant tissue. This would imply that nanoscale changes are a relatively early event in carcinogenesis. This is further supported by our recent report in the MIN mouse model of colon carcinogenesis (20). This model contains a germ-line mutation in the adenomatous polyposis coli tumor suppressor gene, which results in spontaneous polyp formation at ~ 10 weeks. We noted profound changes in $L_d^{(g)}$ and $\sigma^{(g)}$ at 5 weeks that preceded even microadenoma formation, indicating that the genetic alterations in the field carcinogenesis result in structural variations at the nanoscale level that are in turn translated into an increase in disorder strength.

From a biological perspective, these studies do not provide definitive information about the molecular determinants of the disorder strength. However, some insight can be gleaned by our observation that the alterations seem to occur at l_c ~ 50 nm (Δn ~ 0.1; ref. 24). This length scale is well below the diffraction limited resolution of the conventional microscopy, which explains why these cellular changes are not identifiable by conventional histopathology. In addition, the length scale corresponds to the size of some of the most fundamental building blocks of the cell, such as ribosomes, components of cytoskeleton and membranes, etc. Each of these molecular candidate categories has been implicated in the initiation or progression of carcinogenesis. For instance, ribosome dysregulation has long been thought to play a role in carcinogenesis, providing the machinery to increase protein synthesis (25). Many critical proto-oncogenes have been shown to affect ribosomal biogenesis, including c-*Myc* (26). With regard to cytoskeleton, the role is well established in neoplastic transformation including processes such as epithelial-mesenchymal transition (27). Whereas less is known about early events in colon carcinogenesis, it bears emphasis that adenomatous polyposis coli, the initiating mutation in most colorectal cancers, interacts with microtubule structure and has important effect on processes such as chromosomal instability, RNA targeting, etc. (28, 29). Finally,

alterations in membrane proteins and fluidity are well established in early neoplastic transformation of the colon (30). Thus, at the length scale of ~50 nm, there are numerous plausible molecular events, and some or all may be involved in the alterations in disorder strength. Future studies will aim to elucidate the molecular determinants of these changes in nanoscale architecture.

From a clinical perspective, to take the advantage of the field effect detection capabilities of PWS to identify patients at risk for colon carcinogenesis, analysis would need to be done from a readily accessible site. In the colon, this would be the rectum, which is commonly interrogated during physical examination (digital rectal exam). Moreover, it is well established that examination of the rectal mucosa can aid in the prediction of proximal neoplasia. The typical biomarkers to date (aberrant crypt foci, proliferation, apoptosis rates, etc.) have been shown to correlate with proximal neoplasia although the performance characteristics have been inadequate (3, 6, 7). We therefore performed PWS analysis on patients undergoing colonoscopy. Brushings were taken from the endoscopically normal rectal mucosa from 35 patients undergoing complete colonoscopy. In this data set, 20 patients had no neoplasia detected on colonoscopy, 11 patients harbored nonadvanced, and 4 patients had advanced adenomas (defined as adenoma $\geq$1 cm or >25% villous features or presence of high-grade dysplasia). The demographic information such as age, smoking, race, and gender is shown in Table 1. Figure 2*A* to *C* shows that both $L_d^{(g)}$ and $\sigma^{(g)}$ are highly significantly elevated in patients with adenoma compared with the control group (P < 0.001). Interestingly, the patients with advanced adenoma (adenoma >10 mm) had the highest $L_d^{(g)}$ and $\sigma^{(g)}$. Thus, a gradient in the increase of $L_d^{(g)}$ and $\sigma^{(g)}$ in microscopically normal rectal cells parallels the significance of neoplasia. Moreover, if one were to combine the colonic resection and colonoscopy data, the progressive nature is quite striking. Indeed, the $L_d^{(g)}$ of controls (both rectal brushings and benign surgical resections) was 0.3×10^{-5} µm, patients with nonadvanced adenomas were at 0.45×10^{-5} µm, 0.68×10^{-5} µm from those with advanced adenomas, 3.0×10^{-5} µm from uninvolved mucosa of cancer patients, and 3.8×10^{-5} µm for frankly malignant tissue. This is consistent with other field carcinogenesis literature suggesting that the effect size of rectal biomarkers (e.g., aberrant crypt foci) seemed to be greater in patients with more biologically significant lesions.

One question that comes up in the above field carcinogenesis study is whether the PWS signatures [i.e., $L_d^{(g)}$ and $\sigma^{(g)}$] are sensing the presence of neoplasia or simply confounding factors. For instance, age is one of the key risk factors for colonic neoplasia, and there are a variety of age-related changes in the colonic mucosa, including methylation effects that are unrelated to neoplasia. We therefore looked at four of the key demographic risk factors: age, gender, race, and smoking history. As outlined in Table 1, there was no significant difference for age or race. Smoking was increased in patients with advanced adenomas as may be expected because smoking is an established risk factor (portending a ~2- to 3-fold increase risk). We therefore performed an ANCOVA analysis and noted no significant confounding with smoking history [P = 0.50 and P = 0.77 for $L_d^{(g)}$ and $\sigma^{(g)}$, respectively]. Similarly, male gender is a well-established risk factor for colonic neoplasia and was slightly overrepresented among the advanced adenoma patients. However, ANCOVA analysis supported the assertion that there was no significant confounding [P = 0.89 and P = 0.88 for $L_d^{(g)}$ and $\sigma^{(g)}$, respectively]. The correlation analysis further validated the nonsignificant association between the demographic factors and
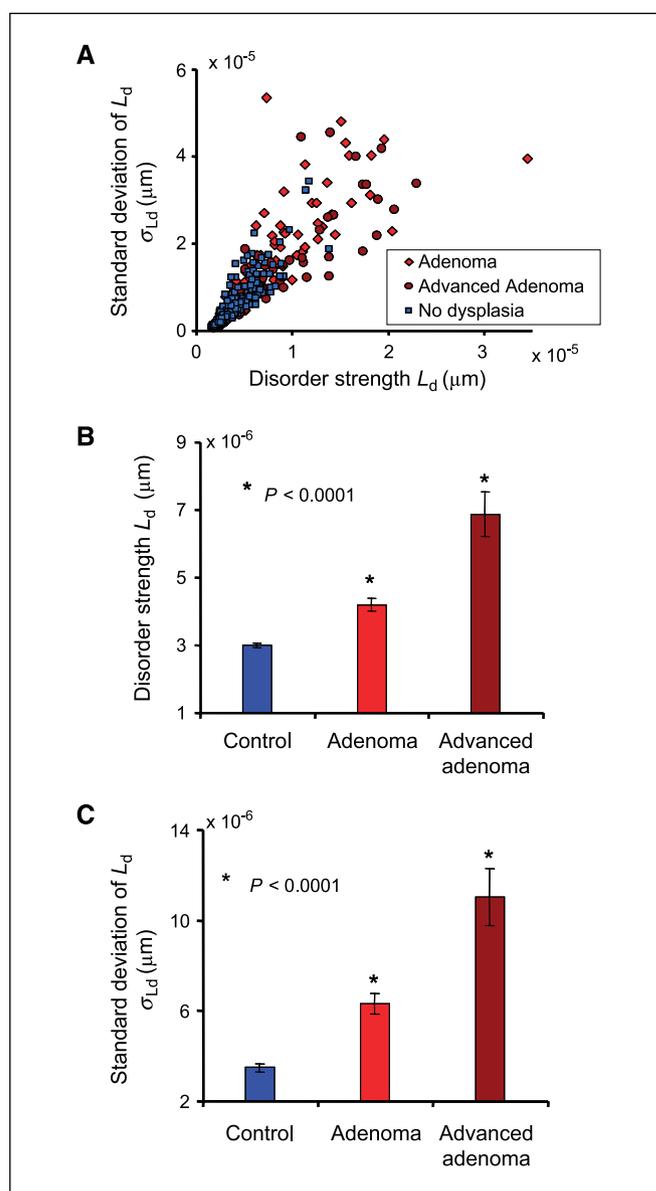

Figure 2. Cells obtained from histologically normal colonic mucosa have increased disorder strength due to the presence of premalignant tumors anywhere else in colon. *A,* values of $L_d^{(c)}$ and $\sigma^{(c)}$ obtained from histologically normal rectal mucosa from control patients and those with adenomatous polyp elsewhere in the colon. Although histologically normal, the rectal cells from patients with premalignant tumors occupy a separate regimen in the parameter space with only slight overlap with the normal cells. *B,* relative values of the disorder strength $L_d^{(g)}$ for cells from histologically normal rectal mucosa in patients with premalignant tumors and those with no tumors present. The average disorder strength $L_d^{(g)}$ is significantly elevated in cells from patients with presence of adenomatous polyps elsewhere in the colon compared with controls (P < 0.0001). *C,* relative values of intracellular SD of the disorder strength $\sigma^{(g)}$ from histologically normal rectal mucosa. $\sigma^{(g)}$ is obtained from ~30 cells for each cell type. *Bars,* SE of the means. Similar to $L_d^{(g)}$, the $\sigma^{(g)}$ is significantly elevated in patients with the presence of premalignant tumors elsewhere in colon (P < 0.0001).

disorder strength parameters. Taken together, these data support the robustness of the association between rectal PWS signatures and colonic neoplasia.

Although the data set is far too small to make any claims about the diagnostic ability, we calculated the performance characteristics to further quantify the robustness of the PWS analysis. The

Table 2. Demographic information of the subjects involved in the pancreatic cancer study and the effect of the patient characteristics on PWS parameters

Demographic factor	Information	Effect on L_d, ANCOVA P	Effect on σ_{Ld}, ANCOVA P
Age (mean $\pm$ SD), y	Control: 61 $\pm$ 11 Cancer: 77 $\pm$ 12	0.72	0.89
Smoking (%smokers)	Control: 50% Cancer: 78%	0.33	0.53
Race (%White)	Control: 89% Cancer: 100%	0.54	0.30
Gender (%male)	Control: 54% Cancer: 33%	0.18	0.26

NOTE: The table indicates that both $L_d^{(g)}$ and $\sigma^{(g)}$ are not confounded by the patient demographic factors.

preliminary estimate of the area under the receiver operator characteristic curve for PWS analysis of rectal brushings was 0.86 for advanced adenoma and 0.76 for all adenomas. For carcinomas (resection studies), the field carcinogenesis effect was 0.90. These estimates do not seem to be overfitted because the area under the receiver operator characteristic curve for all adenomas with leave-one-out cross validation was only minimally decreased to 0.71. We note that the areas under the receiver operator characteristic curve reported were obtained using a single disorder strength parameter of $L_d^{(g)}$ and were not due to the combination of different markers.

Therefore, our data suggest that rectal PWS evaluation may be a powerful means of detecting colonic risk through the identification of field carcinogenesis. We were interested in understanding whether this could potentially be a common theme for many gastrointestinal cancers. In general, gastrointestinal neoplasia is a hallmark of field carcinogenesis. There have been numerous elegant studies on esophageal adenocarcinoma with genetically determined clones detectable (31, 32). Recently, a group reported

that a microarray signature from nonmalignant hepatocytes could predict recurrence in patients who underwent resection with hepatocellular carcinoma, underscoring the role of field carcinogenesis (33). To assess the utility of our paradigm to other gastrointestinal cancers, we chose pancreatic cancer given its lethality (fourth leading cause of cancer deaths among Americans) and lack of a robust screening test. Clinically, the major issue is that instrumenting the pancreatic duct to screen for cancer is not only expensive and uncomfortable but also has a significant incidence of complications ($\sim$5% risk of pancreatitis, which sometimes can be fatal). Our approach was to use the concept of extended field carcinogenesis, which was espoused by Kopelovich and colleagues (34). They noted that for many cancer types, the fingerprint of neoplastic transformation could be detected outside the organ. This may be related to a diffuse field of injury, shared hormonal milieu, or tumor-elaborated factors. For the pancreas, the duodenal mucosa represents a promising target given it is relatively easy and safe to interrogate (via the commonly used tests such as
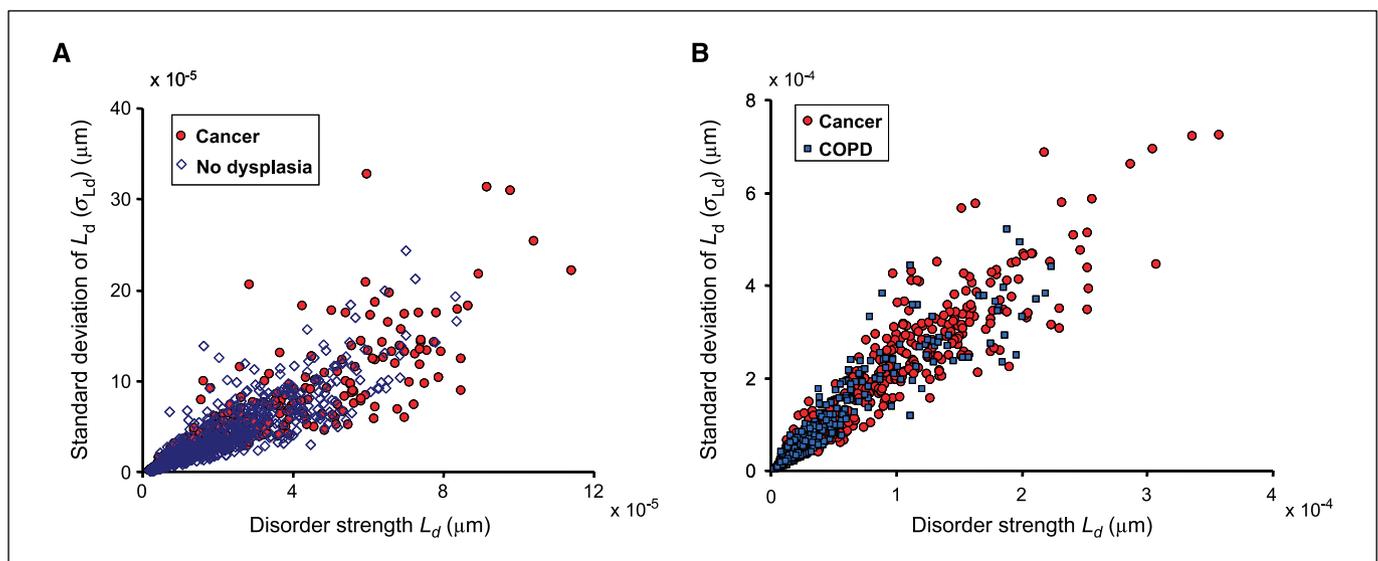

Figure 3. *A,* histologically normal duodenal mucosa cells have increased disorder strength due to the presence of pancreatic cancer. The $L_d^{(c)}$ and $\sigma^{(c)}$ obtained from histologically normal duodenal mucosa from patients with pancreatic cancer and with no cancer. Although histologically normal, the $L_d^{(c)}$ and $\sigma^{(c)}$ from the duodenal cells are significantly elevated in patients with pancreatic cancer ($P < 0.0001$) and the values only slightly overlap with the cells from control patients. *B,* cells obtained from histologically normal buccal mucosa have increased disorder strength due to the presence of lung cancer. Values of $L_d^{(c)}$ and $\sigma^{(c)}$ obtained from histologically normal buccal mucosa from patients with COPD and those with lung cancer. Although histologically normal, the buccal mucosa cells have a much higher $L_d^{(c)}$ and $\sigma^{(c)}$ in patients with lung cancer compared with those patients with COPD ($P < 0.0001$).

Table 3. Demographic information of the subjects involved in the lung cancer study and their effect on PWS parameters

Demographic factor	Information	Effect on L_d, ANCOVA P	Effect on σ_{Ld}, ANCOVA P
Age (mean $\pm$ SD), y	Control: 70 $\pm$ 10 Cancer: 69 $\pm$ 12	0.26	0.36
Smoking (median $\pm$ SD), pack-years	Control: 80 $\pm$ 36 Cancer: 50 $\pm$ 50	0.30	0.30
Race (%White)	Control: 88% Cancer: 90%	0.10	0.18
Gender (%male)	Control: 69% Cancer: 37%	0.35	0.40

NOTE: The table indicates that both $L_d^{(g)}$ and $\sigma^{(g)}$ are not confounded by the patient demographic factors.

---

esophagogastroduodenoscopy). The biological plausibility is underscored by a report by Matsubayashi and colleagues (35) who showed that evaluating the endoscopically normal duodenal mucosa for methylation of important tumor suppressor genes allowed discrimination between patients with pancreatic cancer and chronic pancreatitis. Therefore, we performed brushings on patients with pancreatic cancer (n = 9) and those undergoing upper endoscopy with malignancy (n = 26) and obtained brushings from the endoscopically normal periampullary duodenal mucosa (the demographic information of the patients and their effect on the disorder strength parameters is shown in Table 2). As shown in Fig. 3*A*, the scatter plot shows a marked elevation in both $L_d^{(c)}$ and $\sigma^{(c)}$ of patients with pancreatic cancer when compared with controls (P < 0.0001). This supports the proposition that PWS analysis of field carcinogenesis may be useful for a number of gastrointestinal malignancies.

Finally, we wanted to evaluate whether this concept would translate to malignancies outside the gastrointestinal track. There would be numerous promising candidates (e.g., urogenetic or gynecologic malignancies), but we chose the aerodigestive tract because many feel that it epitomizes field carcinogenesis (36). In particular, lung cancer serves as a nice marker because of the diffuse field of injury from tobacco use. Recent reports from Spira and colleagues (37) suggest genetic alterations in the endoscopically normal right mainstem bronchial epithelium. Whereas the right mainstem bronchus sampling could be viewed as somewhat intrusive, this "field of injury" extends to the buccal (cheek) mucosa (38). Indeed, emerging evidence has suggested that the buccal mucosa may serve as a "molecular mirror" for the lung (39). Given that smoking is the most important risk factor for lung cancer and may alter the oral epithelium, we compared buccal cells from lung cancer patients (n = 18) with those who were cancer-free but had smoked an equivalent amount and thus developed chronic obstructive pulmonary disease (COPD; n = 17). The demographic information of the patients and their effect on $L_d^{(g)}$ and $\sigma^{(g)}$ are given in Table 3. COPD patients were used as a control to avoid confounding by smoking and age. As can be seen from the scatter plot (Fig. 3*B*) there is a clear separation between patients with and without lung cancer (P < 0.0001). Thus, these very preliminary data underscore the promise of this approach in the aerodigestive tract.

These results show that despite being cytologically normal, epithelial cells in the "field" of a tumor have nanoarchitectural changes. Thus, PWS analysis could serve as a marker of field carcinogenesis and hence a novel platform for screening for a

variety of cancers. The clinical imperative for this "pre-screen" is that current clinical practice for cancer screening is inadequate, and thus many patients refuse to undergo recommended screening. For instance, colonoscopy is expensive, intrusive, and has discomfort risks. This is juxtaposed with the observation that the detection rate of significant lesions (advanced adenomas and carcinomas) is only ~ 5%, meaning that 95% of colonoscopies do not have any cancer preventive implications. For lung cancer, no effective population screening option exists with the best candidate, low-dose computerized tomography, hampered by the low prevalence of cancer and high rate of false positives. For pancreatic cancer, computed tomography scans or endoscopic ultrasound are prohibitively cost-ineffective with poor sensitivity to early lesions. Thus, we would envision that assessing field carcinogenesis could serve as an inexpensive, minimally intrusive risk-stratification test analogous to the Pap smear-colposcopy approach that has been so successful in the management of cervical cancer.

In summary, we show herein that using a powerful new light scattering technology, PWS, we are accurately able to detect the nanoscale correlates of field cancerization. In the colon, we show that the effect is not confined to the proximity of the lesion, but can be detected remotely in readily assessable areas such as the rectum. Moreover, the effect size seemed to be proportional to the severity of the neoplastic lesions. Furthermore, this approach has potential applications for other cancers including gastrointestinal and aerodigestive tract cancers. Thus, PWS analysis of field carcinogenesis (both confined to the organ and extended) may serve as a platform for screening for numerous malignancies. Future studies are planned to ascertain the clinical potential of this novel cancer screening paradigm.

Disclosure of Potential Conflicts of Interest

V. Backman, H.K. Roy, and M.J. Goldberg have patent/license interest in partial wave spectroscopy. The other authors disclosed no potential conflicts of interest.

Acknowledgments

References

1. Lewis JD, Ng K, Hung KE, et al. Detection of proximal adenomatous polyps with screening sigmoidoscopy: a systematic review and meta-analysis of screening colonoscopy. Arch Intern Med 2003;163:413–20.

2. Takayama T, Katsuki S, Takahashi Y, et al. Aberrant crypt foci of the colon as precursors of adenoma and cancer. N Engl J Med 1998;339:1277–84.

3. Anti M, Marra G, Armelao F, et al. Rectal epithelial cell proliferation patterns as predictors of adenomatous colorectal polyp recurrence. Gut 1993;34:525–30.

4. Bernstein C, Bernstein H, Garewal H, et al. A bile acid-induced apoptosis assay for colon cancer risk and associated quality control studies. Cancer Res 1999;59: 2353–7.

5. Chen L, Hao C, Chiu Y, et al. Alteration of gene expression in normal-appearing colon mucosa of APCmin mice and human cancer patients. Cancer Res 2004;64:3694–700.

6. Hao CY, Moore DH, Chiu YS, et al. Altered gene expression in normal colonic mucosa of individuals with polyps of the colon. Dis Colon Rectum 2005;48:2329–35.

7. Polley AC, Mulholland F, Pin C, et al. Proteomic analysis reveals field-wide changes in protein expression in the morphologically normal mucosa of patients with colorectal neoplasia. Cancer Res 2006;66:6553–62.

8. Ushijima T. Epigenetic field for cancerization. J Biochem Mol Biol 2007;40:142–50.

9. Alberts DS, Einspahr JG, Krouse RS, et al. Karyometry of the colonic mucosa. Cancer Epidemiol Biomarkers Prev 2007;16:2704–16.

10. Ranger-Moore J, Frank D, Lance P, et al. Karyometry in rectal mucosa of patients with previous colorectal adenomas. Anal Quant Cytol Histol 2005;27:134–42.

11. Anderson PW, Thouless DJ, Abrahams E, Fisher DS. New method for a scaling theory of localization. Phys Rev B 1980;22:3519–26.

12. Kumar N. Resistance fluctuation in a one-dimensional conductor with static disorder. Phys Rev B 1985; 31:5513–5.

13. Rammal R, Doucot B. Invariant imbedding approach to localization. 1. General framework and basic equations. J Phys (Paris) 1987;48:509–26.

14. Pradhan P, Kumar N. Localization of light in coherently amplifying random-media. Phys Rev B 1994; 50:9644–7.

15. Haley SB, Erdos P. Wave-propagation in one-dimensional disordered structures. Phys Rev B 1992;45: 8572–84.

16. Anderson PW. Absence of diffusion in certain random lattices. Phys Rev 1958;109:1492–505.

17. Abrahams E, Anderson PW, Licciardello DC, Ramakrishnan TV. Scaling theory of localization—absence of quantum diffusion in 2 dimensions. Phys Rev Lett 1979;42:673–6.

18. Kramer B, Mackinnon A. Localization—theory and experiment. Rep Prog Phys 1993;56:1469–564.

19. Liu Y, Li X, Kim YL, Backman V. Elastic backscattering spectroscopic microscopy. Opt Lett 2005;30:2445–7.

20. Subramanian H, Pradhan P, Liu Y, et al. Optical methodology for detecting histologically unapparent nanoscale consequences of genetic alterations in biological cells. Proc Natl Acad Sci U S A 2008;105: 20118–23.

21. Subramanian H, Pradhan P, Liu Y, et al. Partial-wave microscopic spectroscopy detects subwavelength refractive index fluctuations: an application to cancer diagnosis. Opt Lett 2009;34:518–20.

22. Bernstein C, Bernstein H, Payne CM, Dvorak K, Garewal H. Field defects in progression to gastrointestinal tract cancers. Cancer Lett 2008;260:1–10.

23. Payne CM, Holubec H, Bernstein C, et al. Crypt-restricted loss and decreased protein expression of cytochrome C oxidase subunit I as potential hypothesis-driven biomarkers of colon cancer risk. Cancer Epidemiol Biomarkers Prev 2005;14:2066–75.

24. Wilson JD, Cottrell WJ, Foster TH. Index-of-refraction-dependent subcellular light scattering observed with organelle-specific dyes. J Biomed Opt 2007;12: 014010.

25. Ruggero D, Pandolfi PP. Does the ribosome translate cancer? Nat Rev Cancer 2003;3:179–92.

26. Dai MS, Lu H. Crosstalk between c-Myc and ribosome in ribosomal biogenesis and cancer. J Cell Biochem 2008;105:670–7.

27. Bazile F, Pascal A, Arnal I, Le Clainche C, Chesnel F, Kubiak JZ. Complex relationship between TCTP, micro-tubules and actin microfilaments regulates cell shape in normal and cancer cells. Carcinogenesis 2009;30:555–65.

28. McCartney BM, Nathke IS. Cell regulation by the Apc protein Apc as master regulator of epithelia. Curr Opin Cell Biol 2008;20:186–93.

29. Mili S, Moissoglu K, Macara IG. Genome-wide screen reveals APC-associated RNAs enriched in cell protrusions. Nature 2008;453:115–9.

30. Brasitus TA, Dudeja PK, Dahiya R, Brown MD. 1,2-Dimethylhydrazine-induced alterations in colonic plasma membrane fluidity: restriction to the luminal region. Biochim Biophys Acta 1987;896:311–7.

31. Brabender J, Marjoram P, Lord RV, et al. The molecular signature of normal squamous esophageal epithelium identifies the presence of a field effect and can discriminate between patients with Barrett's esophagus and patients with Barrett's-associated adenocarcinoma. Cancer Epidemiol Biomarkers Prev 2005;14:2113–7.

32. Maley CC, Galipeau PC, Finley JC, et al. Genetic clonal diversity predicts progression to esophageal adenocarcinoma. Nat Genet 2006;38:468–73.

33. Hoshida Y, Villanueva A, Kobayashi M, et al. Gene expression in fixed tissues and outcome in hepatocellular carcinoma. N Engl J Med 2008;359:1995–2004.

34. Kopelovich L, Henson DE, Gazdar AF, et al. Surrogate anatomic/functional sites for evaluating cancer risk: an extension of the field effect. Clin Cancer Res 1999;5: 3899–905.

35. Matsubayashi H, Sato N, Brune K, et al. Age- and disease-related methylation of multiple genes in non-neoplastic duodenum and in duodenal juice. Clin Cancer Res 2005;11:573–83.

36. Steiling K, Ryan J, Brody JS, Spira A. The field of tissue injury in the lung and airway. Cancer Prev Res 2008;1: 396–403.

37. Spira A, Beane JE, Shah V, et al. Airway epithelial gene expression in the diagnostic evaluation of smokers with suspect lung cancer. Nat Med 2007;13:361–6.

38. Sridhar S, Schembri F, Zeskind J, et al. Smoking-induced gene expression changes in the bronchial airway are reflected in nasal and buccal epithelium. BMC Genomics 2008;9:259.

39. Kemp RA, Turic B. Can early lung cancer be detected from buccal mucosal scrapings? Chest 2005;128:154S.

Cancer Research

The Journal of Cancer Research (1916–1930) | The American Journal of Cancer (1931–1940)

AACR American Association for Cancer Research

Nanoscale Cellular Changes in Field Carcinogenesis Detected by Partial Wave Spectroscopy

Hariharan Subramanian, Hemant K. Roy, Prabhakar Pradhan, et al.

Updated version	Access the most recent version of this article at: doi:10.1158/0008-5472.CAN-08-3895

Cited articles	This article cites 38 articles, 11 of which you can access for free at: http://cancerres.aacrjournals.org/content/69/13/5357.full#ref-list-1
Citing articles	This article has been cited by 12 HighWire-hosted articles. Access the articles at: http://cancerres.aacrjournals.org/content/69/13/5357.full#related-urls

E-mail alerts	Sign up to receive free email-alerts related to this article or journal.
Reprints and Subscriptions	To order reprints of this article or to subscribe to the journal, contact the AACR Publications Department at pubs@aacr.org.
Permissions	To request permission to re-use all or part of this article, use this link http://cancerres.aacrjournals.org/content/69/13/5357. Click on "Request Permissions" which will take you to the Copyright Clearance Center's (CCC) Rightslink site.